Fish and Shellfish Immunology 130 (2022) 223–232

Contents lists available at ScienceDirect

Fish and Shellfish Immunology

journal homepage: www.elsevier.com/locate/fsi

Full length article

Lysine acetylation plays a role in the allograft-induced stress response of the pearl oyster (*Pinctada fucata martensii*)

Jinzhao Lu [a,1], Xiaochen Fang [a,b,1], Haiying Liang [a,c,*], Zhijie Guo [a], Hexin Zou [a]

[a] Fisheries College of Guangdong Ocean University, Zhanjiang, Guangdong, 524088, China
[b] Guangzhou Marine Geological Survey, Guangzhou, Guangdong, 510075, China
[c] Guangdong Provincial Key Laboratory of Aquatic Animal Disease Control and Healthy Culture, Zhanjiang, Guangdong, 524088, China

ARTICLE INFO

Keywords:
Pinctada fucata martensii
Acetylome
Posttranslational modification
Allografting

ABSTRACT

Implanting a spherical nucleus into a recipient oyster is a critical step in artificial pearl production using the pearl oyster *Pinctada fucata martensii*. However, little is known about the role of post-translational modifications (PTMs) in the response of the pearl oyster to this operation. Lysine acetylation, a highly conserved PTM, may be an essential adaptive strategy to manage multiple biotic or abiotic stresses. We conducted the first lysine acetylome analysis of the *P. f. martensii* gill 12 h after nucleus implantation, using tandem mass tags (TMT) labeling and K^{ac} affinity enrichment. We identified 2443 acetylated sites in 1301 proteins, and 1511 sites on 895 proteins were quantitatively informative. We found 25 conserved motifs from all of the identified lysine sites, particularly motifs K^{ac} H, K^{ac} S, and K^{ac} Y were strikingly conserved, of which K^{ac} Y, K^{ac} H, Y K^{ac}, K^{ac} K, K^{ac} *K, K^{ac} R, and K^{ac} F which have been observed in other species and are therefore highly conserved. We identified 58 sites that were significantly differently acetylated in *P. f. martensii* in response to allograft (|fold change|>1.2, *P-value* $\leq$ 0.05); 38 newly acetylated and 20 deacetylated. According to GO functional analysis, subcellar location, and KOG classIfication, these proteins were divided into four categories: cytoskeleton, response to stimulus, metabolism, and other. The differentially acetylated proteins (DAPs) enriched pathways include aminoacyl-tRNA biosynthesis, salmonella infection, and longevity regulating pathway-worm-Caenorhabditis elegans (nematode). Parallel reaction-monitoring (PRM) validation of the differential acetylation of 10 randomly selected differentially acetylated sites from the acetylome analysis. These results indicated that our acetylome analysis results were sufficiently reliable and reproducible. These results provide an essential resource for in-depth exploration of the stress responses and adaptation mechanisms associated with lysine acetylation in marine invertebrates and *P. f. martensii*.

1. Introduction

The pearl oyster, *Pinctada fucata martensii*, is one of the most critical marine bivalves cultured to produce pearls worldwide [1]. In artificial pearl culture, a mantle graft from a donor oyster (the "saibo") and a spherical shell bead (the nucleus) are surgically implanted into the gonad of the recipient or host oyster [2]. These nucleus insertion operations are either xenografts, in which the saibo comes from a species other than the host, or allografts, whenever the saibo originates from a conspecific [3]. The wounds made during transplantation, as well as the foreign substances themselves (i.e., the saibo and nucleus), trigger various immune responses in the host oyster [4]. An effective immune response stimulates the repair of the surgical wounds and removes the pathogens that have entered the oyster during the operation, but an excessively strong immune response can cause transplant rejection or even the host's death [4]. Therefore, the pearl industry must clarify the stress responses and adaptation mechanisms initiated by the host oyster due to nucleus implantation.

Transcriptomic and proteomic studies of the immune response of the recipient oysters have identified, cloned, and functionally characterized several genes and proteins induced in the response of *P. f. martensii* to nucleus implantation [3,5,6], including tumor necrosis factor receptors (TNFR) [2], toll-like receptors (TLRs), interleukin-17 (IL-17) [7], and myeloid differentiation factor 88 (MyD88) [8]. In addition to

* Corresponding author. Guangdong Ocean University, Zhanjiang, Guangdong, PR China.
E-mail address: zjlianghy@126.com (H. Liang).
[1] Jinzhao Lu and Xiaochen Fang contributed equally to the work.

https://doi.org/10.1016/j.fsi.2022.09.018
Received 4 May 2022; Received in revised form 28 August 2022; Accepted 11 September 2022
Available online 17 September 2022

transcription, post-transcriptional regulation, and translation, the immune response also relies on post-translational modifications (PTMs). Indeed, protein PTMs are known to participate in the stress responses of various marine species [9]. For example, a global and site-specific phosphoproteomic analysis of the model cyanobacterium *Synechococcus* sp. PCC 7002 showed that Ser/Thr/Tyr phosphorylation had certain physiological functions, including a two-component signaling pathway and photosynthesis [10], while analysis of hypoxia and reoxygenation in the hypoxia-tolerant marine bivalves *Mytilus edulis*, *Arctica islandica,* and *Crassostrea gigas* showed that reversible phosphorylations on the mitochondrial Complexes I and IV were species- and condition-specific [11]. However, little is known about the PTMs involved in the immune response of *P. f. martensii* to implantation.

Lysine acetylation, a dynamic, reversible, and evolutionarily conserved PTM, consist of the transfer of an acetyl group from acetyl-coenzyme A (acetyl-CoA) to the primary amine in the ε-position of a lysine side chain within a protein [12,13]. Under most physiological conditions, unmodified lysine residues are positively charged, and lysine acetylation neutralizes this charge [14]. Acetylation modification involves biologically essential processes, including transcription, chemotaxis, metabolism, cell signal transduction, stress response, proteolysis, and apoptosis [15–19]. In marine species, it has been hypothesized that lysine acetylation is the primary adaptive response to multiple biotic or abiotic stresses due to its ubiquity and diverse biological functions [9]. In particular, protein acetylation may play a significant role in regulating inflammasome-dependent innate immune responses [9,20]. For example, acetylome analysis of populations of the pacific oyster *C. gigas* suggested that lysine acetylation might be a conserved response to heat stress across marine species [9]. Nonetheless, the analysis of lysine acetylation in *Alvinocaris longirostris* from the deep-sea hydrothermal vents of which was screened for several proteins that may be relevant to stress adaptation, such as arginine kinases, heat shock protein 70, and hemocyanins, of which a total of 9 acetylation sites were detected in two hemocyanin subunits. One of these sites was only present in Alvin's shrimp compared to shallow water shrimp, which may be relevant to adaptation to hypoxia or other environmental stresses [21]. However, the potential involvement of lysine acetylation in the immune response to nucleus implantation into *P. f. martensii* remains uninvestigated. Previous time-series proteomic studies, as well as pearl-insertion technical experience, have shown that 12 h after nucleus insertion marks a critical period of post-grafting stress [22]. Moreover, the gill is a crucial immune organ in mollusks representing the first line of defense against bacterial infection [23].

Thus, to address this knowledge gap, the lysine acetylome of the *P. f. martensii* gill was constructed 12 h after nucleus implantation, and acetylated lysine (K^{ac}) proteins and sites were identified and characterized. Gene ontology (GO) and pathway enrichment analyses suggested that some of the proteins differentially acetylated between the allografted and control individuals were related to cytoskeleton, response to stimulus, metabolism, and others. This study provides critical research for an in-depth exploration of the role of acetylation modifications in the immune response of pearl oysters implantation.

2. Materials and methods

2.1. Sample collection and nucleus implantation

The pearl oysters used (2 years old; shell length approximately 6–8 cm) in this study were collected from the Dajing pearl cultivation base in Xuwen, Zhanjiang, Guangdong province, China. All oysters were acclimatized in tanks kept at 25–27 °C with recirculating natural seawater for one week before the commencement of the experiment. The sample collection procedure is illustrated in Fig. 1. Fifty randomly selected oysters were divided into two groups: the experimental group (ZH12Gi, n = 30), which was over-represented because transplantation may cause death, and the control group (C0Gi, n = 20), in which transplantation did not take place. Nucleus insertion was performed on all oysters in the experimental group in situ by an experienced technician following previous studies [8,9]. Oysters remained in natural seawater throughout the experiment. Gill tissues were pooled to form three replicate samples per group (5 individuals per replicate), yielding three control replicates (C0Gi1, C0Gi2, C0Gi3) and three experimental replicates (ZH12Gi1, ZH12Gi2, ZH12Gi3). All samples were flash-frozen in liquid nitrogen and then stored at −80 °C. An overview of our workflow for this study is

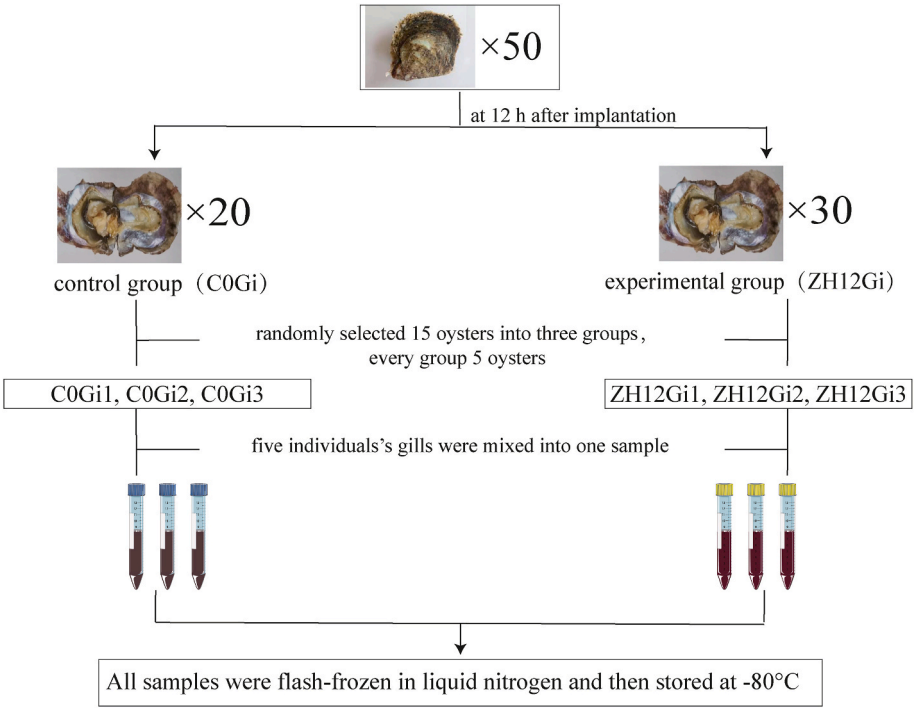

Fig. 1. The sample collection procedure.

shown in Fig. 2A.

2.2. Protein extraction and trypsin digestion

Gill samples were grounded to a powder in liquid nitrogen. Then, four volumes of lysis buffer (8 M urea, 2 mM EDTA, 10 mM dithiothreitol, 1% protease inhibitor cocktail, 3 μM Trichostatin A, 50 mM Nicotinamide) were added to the cell powder, and the mixture was sonicated three times on ice using a high-intensity ultrasonic processor (Scientz, Ningbo, China). Cellular debris was removed by centrifugation at 12,000 g at 4 °C for 10 min. The protein concentration in the supernatant was then determined using a BCA kit (Beyotime, Shanghai, China) following the manufacturer's instructions. To digest the protein, the protein solution was first reduced with 5 mM dithiothreitol for 30 min at 56 °C and alkylated with 11 mM iodoacetamide for 15 min at room temperature in darkness. The sample was then diluted with 100 mM tetraethyl-ammonium bromide (TEAB) to yield a urea concentration of less than 2 M. Finally, trypsin was added at 1:50 trypsin-to-protein mass ratio for the first digestion overnight and then at a 1:100 trypsin-to-protein mass ratio for a second 4 h digestion.

2.3. Tandem mass tag (TMT) labeling

After trypsin digestion, the peptides were desalted using Strata X C18 SPE columns (Phenomenex) and vacuum-dried. Peptides were reconstituted in 0.5 M TEAB and processed for use with the TMT kit (ThermoFisher Scientific, USA), following the manufacturer's protocols. Briefly, one unit of TMT reagent was thawed and reconstituted in acetonitrile. The peptide mixtures were then incubated for 2 h at room temperature and pooled, desalted, and dried using vacuum centrifugation.

2.4. HPLC (high-pressure liquid chromatography) fractionation and affinity enrichment

The tryptic peptides were fractionated by high pH reverse phase HPLC using Thermo Betasil C18 column (5 μm particles, 10 mm ID, 250 mm length). Briefly, peptides were first separated with a gradient of 8%–32% acetonitrile (pH 9.0) over 60 min into 60 fractions. Then, the peptides were combined into 6 fractions and dried by vacuum centrifuging.

To enrich the modified peptides, tryptic peptides dissolved in NETN buffer (100 mM NaCl, 1 mM EDTA, 50 mM Tris-HCl, 0.5% NP-40, pH 8.0) were incubated with pre-washed antibody beads (Lot number 001, PTM Biolabs, Hangzhou, China) at 4 °C overnight with gentle shaking. Then, the beads were washed four times with NETN buffer and twice with H_2O. The bound peptides were eluted from the beads using 0.1% trifluoroacetic acid. The 18 eluted peptide fractions were combined, vacuum-dried, and cleaned for high-resolution liquid chromatography coupled to tandem mass spectrometry (LC-MS/MS) analysis using C18 ZipTips (Millipore), following the manufacturer's instructions.

2.5. LC-MS/MS analysis

The tryptic peptides were dissolved in 0.1% formic acid (solvent A) and directly loaded onto a homemade reversed-phase analytical column (15 cm long, 75 μm i.d.). The LC gradient used was as follows: solvent B (0.1% formic acid in 98% acetonitrile) from 6% to 23% over 26 min, from 23% to 35% over 8 min, from 35% to 80% over 3 min, and then holding at 80% for 3 min. LC was performed on an EASY-nLC 1000 UPLC system (Thermo Scientific, USA) at a constant flow rate of 400 nL/min. The peptides were subjected to nanospray ionization followed by tandem mass spectrometry (MS/MS) using a Q Exactive Plus (Thermo) coupled online to the UPLC. The electrospray voltage was 2.0 kV, the *m/z* scan range was 350–1800 for a full scan, and intact peptides were detected in the Orbitrap at a resolution of 70,000. Peptides were selected for MS/MS using an NCE setting of 28, and fragments were detected in

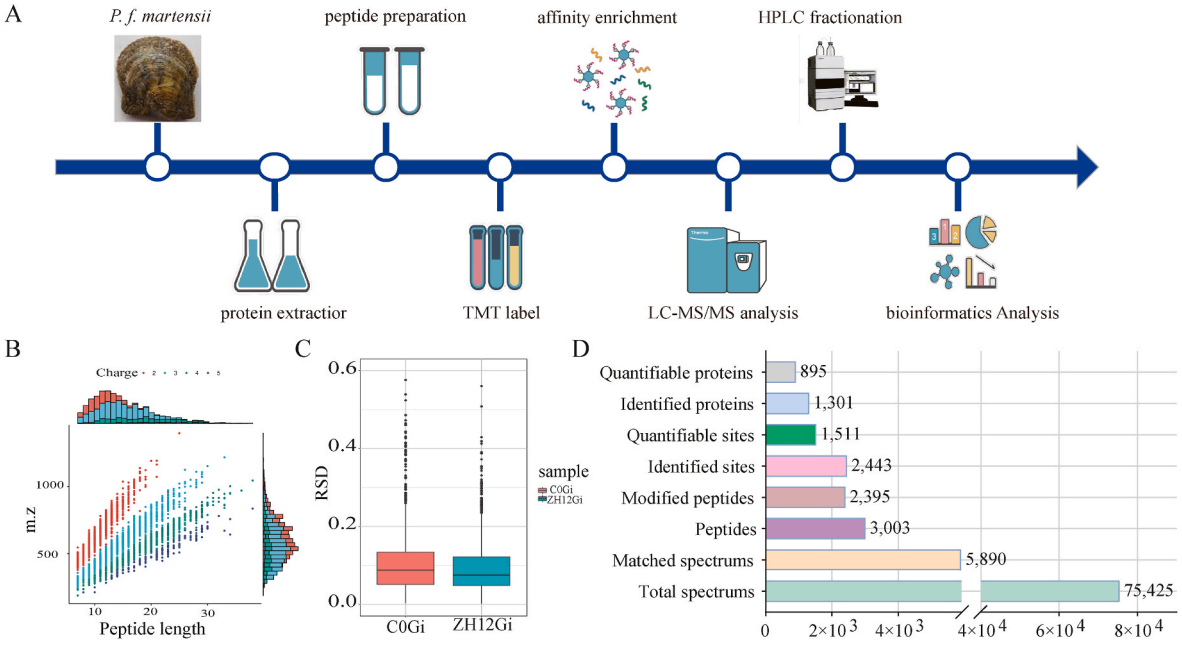

Fig. 2. Summary of the acetylome analysis of *Pinctada fucata martensii*.
(A) The acetylome analysis workflow was used in this study. (B) Peptide length distribution and mass charge ratio (*m/z*) distribution. (C) The relative standard deviation (RSD) was used to test the repeatability of the acetylome sample (D) MS/MS spectrum database search analysis summary (Localization probability >0.75), total spectrum: number of spectrum produced by mass spectrometer; matched spectrum: number of spectrum matched with alignment protein; peptides: number of peptides which spectrum hit; modified peptides: total number of modified peptides identified; identified proteins/sites: number of proteins/modification sites detected by spectrum search analysis; quantifiable proteins/sites: number of proteins/modification sites quantifiable.

the Orbitrap at a resolution of 17,500. We used a data-dependent procedure for MS/MS, in which each MS scan was followed by 20 MS/MS scans with 15.0 s dynamic exclusion. Automatic gain control was set to 5E4, and the fixed first mass was set to 100 *m/z*.

2.6. Database search

The resulting MS/MS data were searched using the Maxquant search engine (v.1.5.1.8) [24]. Tandem mass spectra were searched against the PXD030980 database [22].Trypsin/P was specified as the cleavage enzyme, allowing up to 4 missing cleavages. The mass tolerance for the precursor ions was set to 20 ppm in the first search and 5 ppm in the main search, and the mass tolerance for fragment ions was set to 0.02 Da. Carbamidomethyl on Cys was specified as the fixed modification, while acetylation modification and oxidation on Met were specified as the variable modifications. The false discovery rate (FDR) was adjusted to <1% and the minimum score for modified peptides was set to >40. The quantitative ratio is the ratio of the mean of the three replicates of the experimental (ZH12Gi) and control groups (C0Gi). Furthermore, log2 transform on differentially acetylated proteins quantitative values was first performed, then the two-sample two-tailed *t*-test method was used to calculate *P-value*. Significantly changed protein levels were set as the quantitative ratios >1.2 or <1/1.2 ($P < 0.05$). Four sets of differentially acetylated proteins (DAPs) were constructed: those between the experimental and control group (ZH12Gi/C0Gi) and those between each pair of replicates (ZH12Gi/C0Gi_1; ZH12Gi/C0Gi_2; and ZH12Gi/C0Gi_3). The DAPs (ZH12Gi/C0Gi) clustering results were visualized using a heat map generated using the "heatmap.2" function of the "gplots" R-package [25].

2.7. Bioinformatics analysis

We used the Gene Ontology (GO), Kyoto Encyclopedia of Genes and Genomes (KEGG), InterPro databases, and Wolfpsort soft to annotate protein function, domain function, protein pathway, and subcellular localization, respectively. Soft MoMo (motif-x algorithm) [26] was used to analyze the sequence model composed of amino acids in specific positions of modified 21-mers (10 amino acids upstream and downstream of the modified site) in all protein sequences. When the number of peptides is more significant than 20 ($p < 0.000001$), the sequence is considered a motif of the modified peptide.

The DAPs were categorized into three categories based on GO annotation: biological process, cellular compartment, and molecular function. Eukaryotic Orthologous Group (KOG) analysis was also used to map DAPs (http://genome.jgi.doe.gov/help/kogbrowser.jsf). Furthermore, the KEGG database was used to identify pathways in which the obtained DAPs are enriched. InterPro functionally analyzes protein sequences by classifying them into families and predicting the presence of domains and important sites. In a further enrichment analysis based on DAPs functional classification (such as GO, domain, and pathway), we employed a two-tailed Fisher's exact test to test the enrichment of the DAPs against all identified proteins; a corrected *p-value* < 0.05 was considered significant.

2.8. Targeted parallel reaction monitoring (PRM) analysis of validation of selected DAPs

We randomly selected 8 DAPs, including 10 Kac sites, for PRM quantification, performed by PTM Biolabs (Hangzhou, China). Consequently, protein extraction, trypsin digestion, as well as affinity enrichment were prepared as described for TMT (see sections 2.2 and 2.4).

The peptides were dissolved in solvent A (0.1% formic acid 2% acetonitrile) and directly loaded onto a homemade reversed-phase analytic column. The gradient used was as follows: solvent B (0.1% formic acid in 98% acetonitrile) from 6% to 23% over 38 min, from 23% to 35% over 14 min, from 35% to 80% over 4 min, and then holding at 80% for 4 min. LC was performed on an EASY-nLC 1000 UPLC system at a constant flow rate of 700 nL/min. The peptides were subjected to nanospray ionization followed by tandem mass spectrometry (MS/MS) using a Q ExactiveTM Plus (Thermo) coupled online to the UPLC. The electrospray voltage was 2.0 kV, the *m/z* scan range was 350–1000 for a full scan, and intact peptides were detected in the Orbitrap at a resolution of 35,000. Peptides were selected for MS/MS using an NCE setting of 27, and fragments were detected in the Orbitrap at a resolution of 17,500. We used a data-dependent procedure for MS/MS, in which each MS scan was followed by 20 MS/MS scans with 15.0 s dynamic exclusion. Automatic gain control was set to 3E6 for the entire MS and 1E5 for MS/MS. The maximum IT was set to 20 ms for the entire MS and auto for MS/MS. The isolation window for MS/MS was set to 2.0 *m/z*.

The resulting MS data were processed using Skyline (v.3.6) [27]. The peptide settings were as follows: enzyme was set to Trypsin [KR/P], max missed cleavage was set to 2, and peptide length was set to 8–25. The variable modifications were set to Carbamidomethyl on oxidation and Cys on Met, and the max variable modifications were set to 3. The transition settings were as follows: the precursor charges were set to 2, 3; the ion charges were set to 1, 2; and the ion types were set to b, y, p. Production was set from ion 3 to the last ion, and the ion match tolerance was set to 0.02 Da.

3. Results

3.1. Quality control validation of the MS data

Fig. 2A depicts an overview of the experimental procedure. We began by examining the lysine acetylome's quality. Most peptides were 7–20 amino acids long, typical of tryptic peptides (Fig. 2B), indicating that sample preparation was adequate. Furthermore, the study plotted box plots using the relative standard deviation (RSD) of the protein quantification values between replicates (Fig. 2C). The lower the overall RSD value, the better the sample's reproducibility. The MS/MS data search identified 2443 acetylated sites in 1301 proteins, of which 1511 sites on 895 proteins were quantitatively informative (Fig. 2D).

3.2. Analysis of the acetylated lysine sites

To better understand the properties of the identified sites and peptides in *P. f. martensii* after allografting, we performed a motif analysis to calculate the positions surrounding the acetylation site (−10 to +10 amino acids). Twenty-five conserved motifs were found from all of the identified K^{ac} sites, including K^{ac}N, YK^{ac}N, K^{ac}ND, K^{ac}YP, GK^{ac}S, PK^{ac}N, AK^{ac}N, RK^{ac}S, FK^{ac}N, K^{ac}YQ, LK^{ac}N, QK^{ac}Y, K^{ac}H, K^{ac}Y, K^{ac}S, K^{ac}F, K^{ac}N, K^{ac}W, YK^{ac}, GK^{ac}, FK^{ac}, K^{ac}R, K^{ac}K, K^{ac}T, and K^{ac} *K (* represents a random amino acid residue, Fig. 3A). Particularly motifs K^{ac}H, K^{ac}S, and K^{ac}Y were strikingly conserved (Fig. 3B). A heat map of amino acid composition surrounding the acetylated lysine revealed that glycine (G), tyrosine (Y), and alanine (A) were over-represented in positions −1 to −4, while serine (S), glutamic acid (E), and lysine (K) were the least enriched in those positions, with A appearing only rarely at positions +1 and + 2; E was rarely appeared at +1 and −1; phenylalanine (F), histidine (H), tryptophan (W) and Y occurred most frequently at +1; by contrast, and glutamine (Q) had the lowest frequency at position +1, while the occurrence of serine (S) enriched was only at position +1 (Fig. 3C). The results show a preference for certain amino acids upstream and downstream of the post-implantation acetylation modification site in *P. f. martensii*.

3.3. Differential patterns of acetylation in pearl oysters after allografting

Across the three sets of replicates (ZH12Gi/C0Gi_1; ZH12Gi/C0Gi_2; and ZH12Gi/C0Gi_3), we identified an average of 33 significantly differentially acetylated sites and 14 significantly differentially

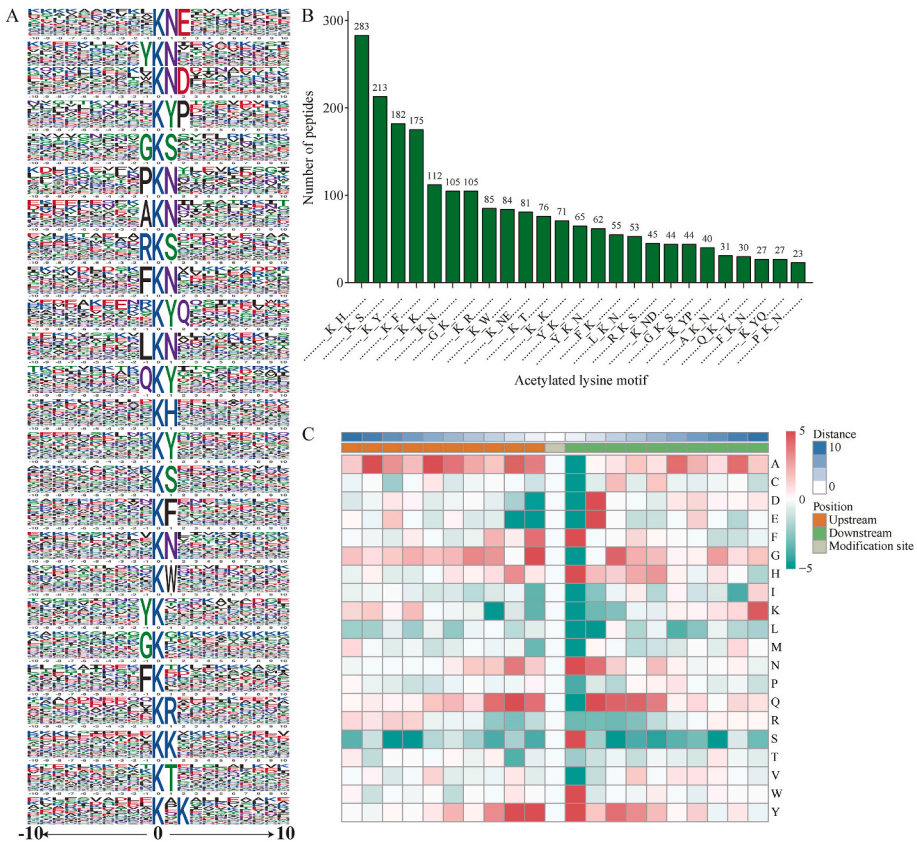

Fig. 3. Motifs surrounding the identified acetylated lysine (K^{ac}) sites in *Pinctada fucata martensii*. (A) Conserved motifs surrounding the K^{ac} sites. Letters correspond to amino acid residues, and the size of the letter reflects the frequency of that amino acid residues in that position. (B) The number of peptides identified in each conserved motif. (C) Heatmap showing amino acid frequencies surrounding K^{ac} sites; red cells correspond to the enrichment of the amino acid in that position, while green cells indicate the reverse.

acetylated proteins (fold change >1.2 or < 1/1.2, $P \leq 0.05$; Fig. 4A). In total, 58 sites were differently acetylated between allografted oysters and the control oysters; acetylation increased at 38 sites in 33 proteins and decreased at 20 sites in 14 proteins.

The repeated changes in acetylation in six samples were the focus of this study. We conducted a GO functional analysis, subcellar location, and KOG classification to obtain an overview of the DAPs after allografting. The GO terms overrepresented in the DAPs included the biological process terms "cellular process" (28 proteins), "biological regulation" (21 proteins), and "metabolic process" (19 proteins); the cellular component term "cell" (23 proteins); and the molecular function term "binding" (18 proteins) and "catalytic activity" (15 proteins; Fig. 4B). In further analyzing the precise location of DAPs, the results showed that DAPs in the gill was mainly localized in the cytoplasm (42.55%), nucleus (21.28%), and mitochondria (12.77%, Fig. 4C). KOG analysis indicated that most of the differentially regulated acetylated proteins were associated with cellular processes and signaling (20 proteins) or information storage and processing (14 proteins), including translation, ribosomal structure and biogenesis, and the cytoskeleton (Fig. 4D).

According to functional classification, these proteins were divided into four categories: cytoskeleton, response to stimulus, metabolism, and other. We used hierarchical clustering based on differently modified change quantitative, the result indicates that acetylation might serve different functions. Acetylation can serve multiple functions on the same category of protein (Fig. 5). Most proteins involved in metabolism and response stimulus were acetylated, such as related to response stimulus proteins, including E3 ubiquitin-protein ligase MIB2, Zinc metalloproteinase (nas-15), 60 kDa heat shock protein (HSPD1), and Complement C1q-like protein 3 (C1ql3), and related to metabolism proteins including Cysteine–tRNA ligase (Cars), Pyruvate dehydrogenase E1 component subunit beta (Pdhb), Tryptophan–tRNA ligase (WARS) were up-regulated acetylated. Several metabolism-related proteins were deacetylated, including Transketolase-like protein 2 (Tktl2), Fatty acid-binding protein 5 (FABP5), and Isoleucine—tRNA ligase (IARS). Both acetylated and deacetylated proteins associated with the cytoskeleton were found. In this case, several myosin-heavy chain sites were deacetylated.

3.4. Functional enrichment of the DAPs

Enrichment tests were performed on the data further to clarify the cellular functions of these DAPs after allografting. GO-based enrichment analysis revealed that in the classification of biological processes, "circadian regulation of gene expression," "regulation of stem cell differentiation," and "circadian regulation of gene expression" were significantly enriched (Fig. 6A), whereas in the molecular function category, "double-stranded RNA binding," "RNA polymerase binding," and "ligase activity were significantly enriched (Fig. 6B). On the other hand, the significantly enriched DAPs in the cellular component category were primarily "apical dendrite," "dendritic shaft," and "histone acetyltransferase complex" (Fig. 6C). The protein domains significantly enriched in the DAPs were "Transketolase, C-terminal domain," "Transketolase, pyrimidine binding domain," "Astacin (Peptidase family M12A)," and "Calponin homology (CH) domain" (Fig. 6D).

KEGG pathway enrichment analysis showed that the pathways enriched in the differentially acetylated proteins included aminoacyl-tRNA biosynthesis (KEGG: map00970), salmonella infection (KEGG: map05132), and longevity regulating pathway-worm-Caenorhabditis elegans (nematode) (KEGG: map04212) (Fig. 6E). It is worth noting that WARS, IARS, and Cars were involved in the aminoacyl-tRNA biosynthesis pathway; probable ATP-dependent RNA helicase DDX58, Probable actin-related protein 2/3 complex subunit 2 (Arc-p34), and Filamin-C(FLNC) were involved salmonella infection pathway; HSPD1 and protein mono-ADP-ribosyltransferase PARP3 were involved longevity regulating pathway-worm-Caenorhabditis elegans

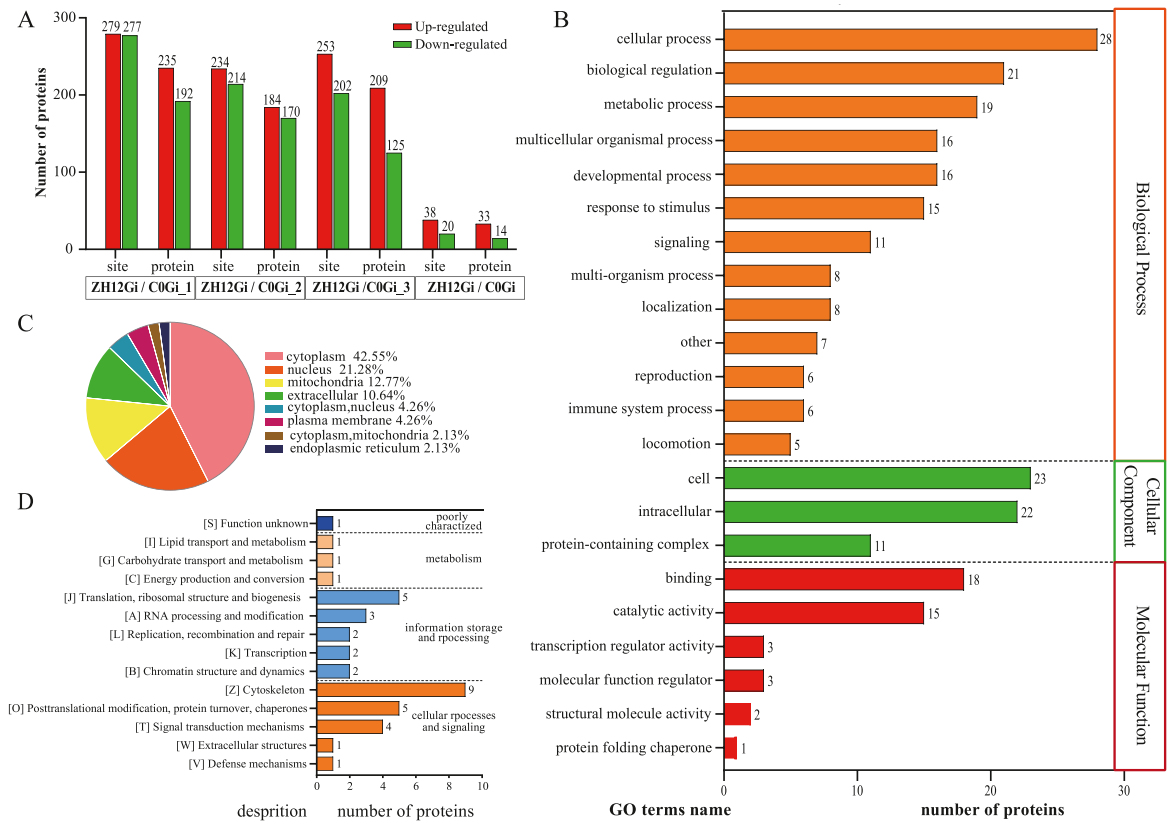

Fig. 4. Functional enrichment of differentially acetylated proteins (DAPs) in *Pinctada fucata martensii* in response to the allograft.
(A) Differentially acetylated sites and proteins identified between pairs of replicates (ZH12Gi/C0Gi_1; ZH12Gi/C0Gi_2; and ZH12Gi/C0Gi_3) and between the experimental and control groups as a whole (ZH12Gi/C0Gi) after allograft. (B) The classification of DAPs in biological process, cellular component, and molecular function. The number of proteins in which each corresponding term is enriched is given to the right of the bar. (C) The subcellular locations of the DAPs. (E) KOG functional classification of the DAPs.

(nematode).

3.5. PRM data validation

In this study, 9 DAPs were chosen for PRM analysis to confirm the data's accuracy (Table 1). PRM is a "targeted" mass spectrometry technique that can verify many proteins and has been used to assess quantitative differences between biological samples in recent years. PRM validation of the differential acetylation of 10 randomly selected differentially acetylated sites from the acetylome analysis (Table 1). These results indicated that our acetylome analysis results were sufficiently reliable and reproducible.

4. Discussion

Although acetylation is thought to regulate organismal homeostasis during the initial stress response in most animals, little is known about its role in marine species [9]. Furthermore, the balance of acetylation/deacetylation is important in regulating inflammation [28]. Many transcriptomics and proteomics studies have been carried out in pearl oysters to look into the early stages of grafting adaptation and molecular mechanisms responses. To solve the scientific problem, post-translational modifications of proteins are just as significant as changes in the protein content of genes. However, there is still a knowledge gap in protein acetylation modification after allografting. Therefore, we constructed the quantitative acetylome from the gill tissue of *P. f. martensii* at 12 h after allografting, the first study of the immune response of the oyster pearl at the level of post-translational modifications.

Here, we identified 2443 acetylated sites in 1301 proteins, of which 1511 sites on 895 proteins contained quantitative information. The locations surrounding the acetylation site of the identified sites and peptides were calculated using a motif analysis. There, we found 25 conserved motifs from all of the identified lysine sites, such as $K^{ac}Y$ [21, 29–32], $K^{ac}H$ [31], YK^{ac} [32], $K^{ac}K$ [33,34], K^{ac} *K [34,35], $K^{ac}R$ [34, 35], and $K^{ac}F$ [36] were found in other species and hence are highly conserved across organisms. The conserved amino acid motifs surrounding the acetylated sites included a preference for G at position −1, and low frequencies of G in position +1. Consistent with previous studies, G and Y were the more common residues in the vicinity of the acetylation modification site [37], of which G at position −1 has been previously identified as part of a recognition motif for the nuclear CBP/p300 lysine acetyltransferase complex [38]. In alkaline amino acids, a very high frequency of H at position +1 was found in the plants [39,40], bacteria [41], and the invertebrate *C. gigas* [9]and *A. longirostris*, which shows consistency. Moreover, consistent with *C. gigas* in response to heat stress, A occurs more frequently at several upstream and downstream sites but less frequently at the +1 position [9]. Consistent with *A. longirostris* and *Apostichopus japonicus*, the aromatic amino acids Y and F occur more frequently at position +1 [21,42]. These results suggested that lysine acetylation may be a conserved modification in different species. However, inconsistently with the *A. longirostris*, arginine and K do not occur as frequently at the position +1 [21]. It may indicate that proteins carrying these motifs have specific functions in *P. f. martensii* responding to allograft-induced stress.

In total, 58 sites were differently acetylated (38 sites newly acetylated and 20 sites deacetylated) across all three replicates. There were substantial differences in the patterns of differential acetylation among

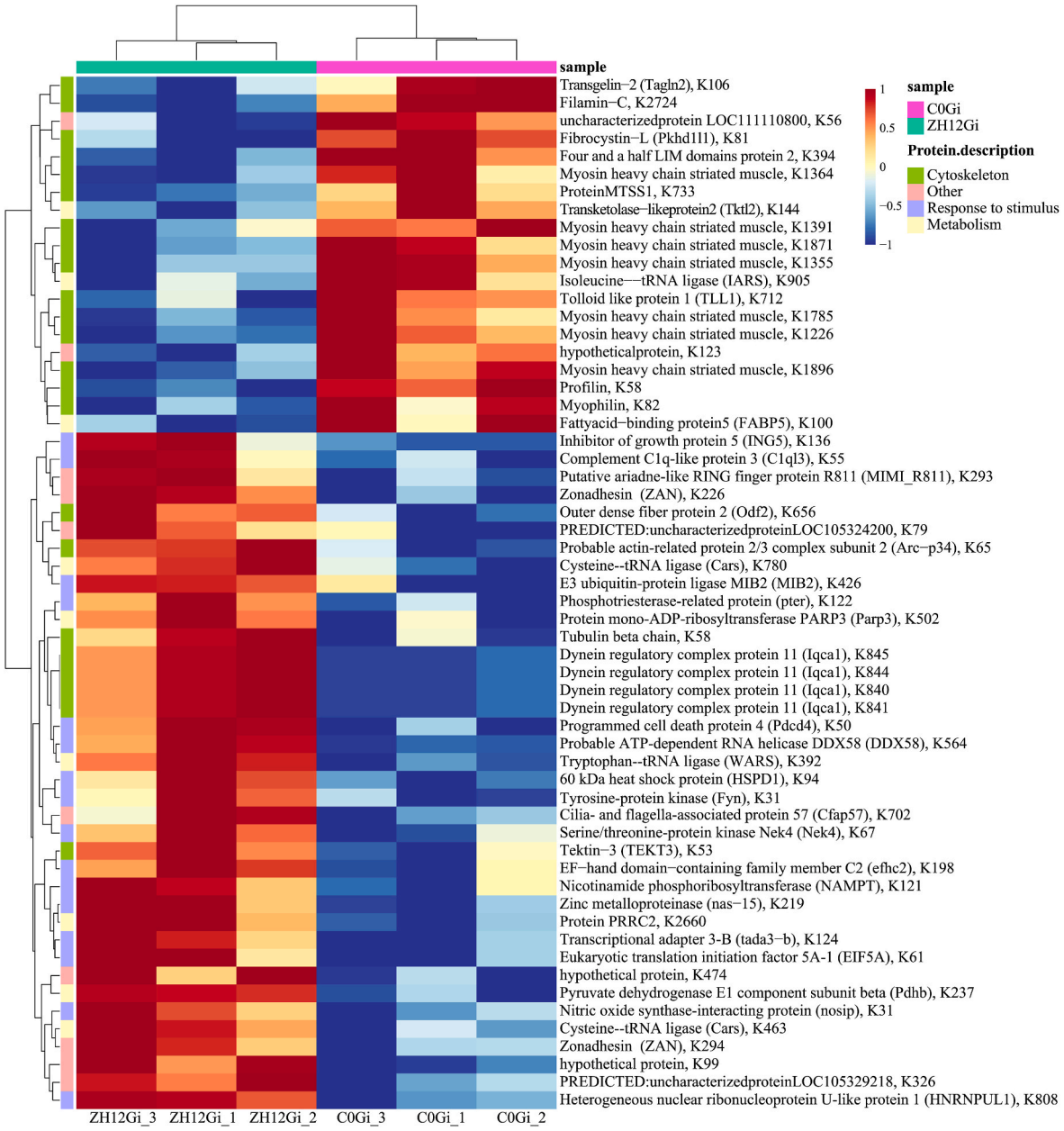

Fig. 5. A heat map of differently modified sites.
The clustering was constructed using the complete-linkage method together with the Euclidean distance. Higher z-scores and thus higher relative modified abundances for each protein are represented by the red color. A z-score of 0 indicates that the protein abundance value is equal to the average of all abundance values for that protein. Each row represents a differentially modified protein (DAP) and each column, a sample. The DAPs clustering tree was on the right, while the samples clustering tree was on the up.

replicate pairs, implying that it was possibly related to dynamic and reversible lysine acetylation modification and variance in individuals of *P. f. martensii*. These proteins were grouped into four categories based on their functional classification: cytoskeleton, reaction to stimulus, metabolism, and others. Among these differently acetylated proteins, myosin heavy chains were highly acetylated (more acetylation sites), which is consistent with the gill of *C. gigas* [9], and PRM had confirmed two sites. Previous studies have revealed that acetylation of myosin heavy chains modulates actin-activated ATPase activity and actin-sliding velocity of cardiac myosin [43,44]. Moreover, the salmonella infection KEGG pathway is characterized by rearranging the actin cytoskeleton to promote pathogen uptake into host cells and its subsequent proliferation and intercellular spread, thereby enhancing virulence [45]. It may indicate that cytoskeleton protein acetylation is related to the allografting of *P. f. martensii*.

In KOG and GO classification, many DAPs were associated with cellular processes and signaling or information storage and processing and response to stimulus or immune system. The longevity regulating pathway-worm-Caenorhabditis elegans (nematode) pathway was related to aging, which was used to resist a complex process of accumulation of molecular, cell, and even organ damage leading to loss of function and increased vulnerability to disease and death [46]. Of which HSPD1 enriched the pathway. HSPs are conserved molecular chaperones that inhibit protein misfolding, participate in apoptosis, and play a role in the immune response to stress [47]. Consistent with this, a previous study showed that HSPD1 was strongly up-regulated 12 h after LPS stimulation in *P. f. martensii* [48], indicating that external antigens may induce HSP60 expression and thus the stress response, implying that the

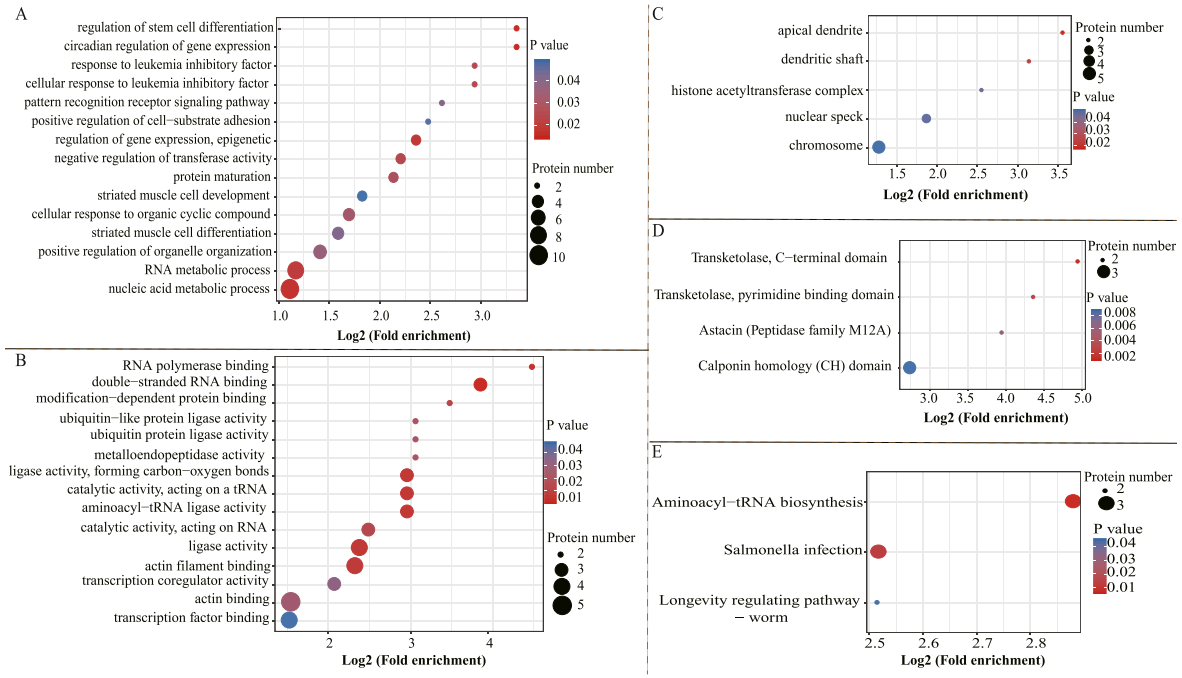

Fig. 6. Enrichment of gene ontology (GO) terms, protein domains, and KEGG pathways in the differentially acetylated proteins (DAPs) in *Pinctada fucata martensii* in response to the allograft.
(A–C) The GO terms are enriched in the DAPs: (A) biological process terms, (B) molecular function terms, and (C) cellular component terms. (D) The protein domains are enriched in the DAPs. (E) KEGG pathways were significantly enriched in the DAPs. Point size and color reflect the number of proteins enriched in the corresponding pathway and the q-value; larger enrichment values with lower q-values indicate a greater degree of enrichment.

Table 1
Validation of DAPs using parallel reaction monitoring (PRM) analysis.

Protein Accession	Protein description	Protein Gene	Position	ZH12Gi/ C0Gi Ratio (PRM)	ZH12Gi/C0Gi P Value (PRM)	ZH12Gi/C0Gi Ratio (TMT)	ZH12Gi/ C0Gi P value (TMT)
TRINITY_DN119_c0_g1_m.1367	uncharacterized protein LOC105324200	–	79	3.34	0.00	2.203	0.043
TRINITY_DN5852_c0_g1_m.12,144	Nitric oxide synthase-interacting protein	nosip	31	1.69	0.31	1.47	0.026
TRINITY_DN4405_c0_g1_m.9938	Zonadhesin	ZAN	226	1.76	0.00	1.946	0.0041
TRINITY_DN4405_c0_g1_m.9938	Zonadhesin	ZAN	294	1.72	0.01	1.751	0.038
TRINITY_DN1761_c0_g1_m.3893	Four and a half LIM domains protein 2	FHL2	394	0.73	0.03	0.767	0.0036
TRINITY_DN55970_c0_g1_m.11,789	Complement C1q-like protein 3	C1ql3	55	1.52	0.01	1.366	0.037
TRINITY_DN122_c0_g1_m.1541	Myosin heavy chain	–	1226	0.49	0.00	0.771	0.0091
TRINITY_DN122_c0_g1_m.1541	Myosin heavy chain	–	1391	0.57	0.00	0.772	0.039
TRINITY_DN3859_c0_g1_m.8997	Tubulin beta chain	–	58	1.32	0.04	1.289	0.028
TRINITY_DN757_c0_g1_m.14,231	Cysteine–tRNA ligase	Cars	463	1.99	0.03	1.51	0.021

HSP60 gene is involved in immunological stress. Additionally, the PTM of HSP60 (specifical acetylation) has been observed in several cancers, including lung cancer, in which HSP60 acetylation inhibited the interaction between p53 and HSP60, and osteosarcoma, in which the hyperacetylated HSP60 mitochondrial protein-induced cell apoptosis [47]. Although acetylation of HSP60 has been proposed to contribute to its degradation [49], this was not identified in the proteome of *P. f. martensii* gills 12 h after nucleus implantation [22]. As a result, the involvement of HSP60 acetylation alteration in allografting has to be investigated further. Moreover, proteins with C1q domains play an important role in triggering the classical complement pathway, a prominent effector mechanism in the innate immune system. C1q is involved in the innate immune response in *P. f. martensii*, as well as shell formation and antibacterial activity in vitro [50–52]. Here, PRM confirmed that C1ql3 is differently modified in K55. Therefore, the impact of acetylation of C1ql3 at this location on its function and involvement in allografting has to be investigated further. These results suggest that protein acetylation associated with reaction stimulus may be related to allografting in *P.f. martensii*.

Aminoacyl-tRNA biosynthesis was shown to have significant enrichment in the KEGG database, including WARS, IARS, and Cars. It has been proven that enhanced amino acid catabolism, such as low water temperature stress [53], larval metamorphosis [54], and implantation [22], are common responses to inflammation. Furthermore, the route of aminoacyl-tRNA production was significantly enriched in transcriptome analyses of shell damage repair [57] and reduced transcription factor PmRunt [58]. Likewise, metabolism-related GO entries were significantly enriched, suggesting that regulating metabolic processes is critical to the immune response of the implantation of pearl oysters. In addition, Pdhb and Tktl2 are essential rate-limiting enzymes in the tricarboxylic acid cycle (TCA) and the pentose phosphate pathway (PPP), respectively. When there is a lack of oxygen, such as in cancer

cells, hypoxia-inducible factor-1 promotes ribose synthesis for the nucleic acid anabolic pathway by up-regulating the expression of transketolase (TKT) and TKTL2 genes and inhibits pyruvate dehydrogenase from increased reactive oxygen species generation in mitochondria [55]. Enzymatic or non-enzymatic action, metabolic enzymes can create reversible acetylation changes, impacting enzyme performance and stability [56]. According to previous research, SIRT3 interacts with the pyruvate dehydrogenase E1 to increase its enzymatic activity by deacetylation, which can increase oxidative phosphorylation and reactive oxygen species (ROS) production while decreasing glycolysis [57]. Oyster pearl air exposure raised CO_2 concentration and lowered pH [58], and stress in shellfish increases the generation of ROS, which might explain the changed acetylation modification of Tktl2 and Pdhb. These results suggest a link between nucleus implantation and metabolism in *P. f. martensii*.

In our previous study, comparative proteomics and transcriptomics analysis after a 12-h allograft in *P. f. martensii*, showed that changes in transcriptome data do not always correspond to changes in protein expression [22]. We looked at post-translational acetylation changes to better understand the pearl oyster's allograft-induced stress response. On the one hand, we discovered specific proteins involved in the cytoskeleton, reaction to stimulus, metabolism, and other processes. However, the specific roles of essential proteins in the allograft response remain to be explored, especially the effects of protein acetylation levels on protein function. Additionally, these studies may provide novel intervention targets clearly and offer practical advice for the rational control of the pearl oyster immune response.

5. Conclusion

Lysine acetylation, a highly conserved PTM, may be an essential adaptive strategy used by marine species to manage multiple biotic or abiotic stresses. Here, we analyzed the response of *P. f. martensii* to allograft using TMT labeling and K^{ac} affinity enrichment. We identified 2443 acetylated sites in 1301 proteins, of which 1511 sites on 895 proteins were quantitatively informative. There was substantial variation in acetylation patterns among replicates: only 58 sites were differentially acetylated in response to allograft across all three replicates (38 sites newly acetylated and 20 sites deacetylated). Here, we found 25 conserved motifs from the identified lysine sites; some of them were strikingly conserved and have been observed in other species. These findings show that lysine acetylation may be a conserved PTM. We conducted a GO functional analysis, subcellar location, and KOG classification to obtain an overview of the DAPs after allografting. According to functional classification, these proteins were divided into four categories: cytoskeleton, response to stimulus, metabolism, and other. Myosin heavy chains were substantially acetylated (more acetylation sites) among these DAPs, with the majority of sites deacetylated and two sites verified by PRM. KEGG pathway enrichment analysis showed that the pathways enriched in the DAPs included aminoacyl-tRNA biosynthesis, salmonella infection, and longevity regulating pathway-worm-Caenorhabditis elegans (nematode). However, the specific roles played by these acetylated proteins and acetylation, in general, in the response of *P. f. martensii* to allografts remain to be investigated. Our results provide new protein targets for functional studies and, in addition, represent an important resource for the in-depth exploration of the stress responses and adaptative mechanisms associated with lysine acetylation in marine invertebrates and *P. f. martensii* in particular.

CRediT authorship contribution statement

Jinzhao Lu: Supervision, Formal analysis, Writing – original draft. **Xiaochen Fang:** Formal analysis. **Haiying Liang:** Conceptualization, Methodology, Writing – review &; editing. **Zhijie Guo:** prepared the samples. **Hexin Zou:** Validation.

Data availability

Data will be made available on request.

Acknowledgments

This work was supported by the grants from the National Natural Science Foundation of China (No. 31472306), Guangdong Provincial Natural Science Foundation (No. 2021A1515010962), Special Fund Project for Science and Technology Innovation Strategy of Guangdong Province (2021A05250), Special Fund for Harbor Construction and Fishery Industry Development of Guangdong Province (No. A201608B15) and Sustainable Development Project of Shenzhen Science and Technology Program (KCXFZ20211020165547010).

We thank Dr. Amoah Kwaku for linguistic assistance and pre-submission expert review.

References

[1] J. He, C. Shen, H. Liang, et al., Antimicrobial properties and immune-related gene expression of a C-type lectin isolated from *Pinctada fucata martensii*, Fish Shellfish Immunol. 105 (2020) 330–340, https://doi.org/10.1016/j.fsi.2020.07.017.
[2] Y. Wu, J. He, G. Yao, et al., Molecular cloning, characterization, and expression of two TNFRs from the pearl oyster *Pinctada fucata martensii*, Fish Shellfish Immunol. 98 (2020) 147–159, https://doi.org/10.1016/j.fsi.2020.01.010.
[3] Y. Jiao, S. Yang, Y. Cao, et al., Genome and transcriptome analyses providing insight into the immune response of pearl oysters after allograft and xenograft transplantations, Fish Shellfish Immunol. 90 (2019) 109–117, https://doi.org/10.1016/j.fsi.2019.04.061.
[4] L. Adzigbli, R. Hao, Y. Jiao, et al., Immune response of pearl oysters to stress and diseases, Rev. Aquacult. 12 (2020) 513–523, https://doi.org/10.1111/raq.12329.
[5] W. Wang, Y. Wu, Q. Lei, et al., Deep transcriptome profiling sheds light on key players in nucleus implantation induced immune response in the pearl oyster *Pinctada martensii*, Fish Shellfish Immunol. 69 (2017) 67–77, https://doi.org/10.1016/j.fsi.2017.08.011.
[6] W. Wang, Q. Lei, H. Liang, et al., Towards a better understanding of allograft-induced stress response in the pearl oyster *Pinctada fucata martensii*: insights from iTRAQ-based comparative proteomic analysis, Fish Shellfish Immunol. 86 (2019) 186–195, https://doi.org/10.1016/j.fsi.2018.11.044.
[7] Y. Cao, S. Yang, C. Feng, et al., Evolution and function analysis of interleukin-17 gene from *Pinctada fucata martensii*, Fish Shellfish Immunol. 88 (2019) 102–110, https://doi.org/10.1016/j.fsi.2019.02.044.
[8] Y. Jiao, Z. Gu, S. Luo, et al., Evolutionary and functional analysis of MyD88 genes in *pearl oyster Pinctada fucata martensii*, Fish Shellfish Immunol. 99 (2020) 322–330, https://doi.org/10.1016/j.fsi.2020.02.018.
[9] A. Li, L. Li, W. Wang, et al., Acetylome analysis reveals population differentiation of the pacific oyster *Crassostrea gigas* in response to heat stress, Mar. Biotechnol. 22 (2020) 233–245, https://doi.org/10.1007/s10126-020-09947-6.
[10] M.-k. Yang, Z.-x. Qiao, W.-y. Zhang, et al., Global phosphoproteomic analysis reveals diverse functions of serine/threonine/tyrosine phosphorylation in the model cyanobacterium Synechococcus sp. strain PCC 7002, J. Proteome Res. 12 (2013) 1909–1923, https://doi.org/10.1021/pr4000043.
[11] H.I. Falfushynska, E. Sokolov, H. Piontkivska, et al., The Role of Reversible Protein Phosphorylation in Regulation of the Mitochondrial Electron Transport System during Hypoxia and Reoxygenation Stress in Marine Bivalves, vol. 7, 2020, https://doi.org/10.3389/fmars.2020.00467.
[12] I. Ali, R.J. Conrad, E. Verdin, et al., Lysine acetylation goes global: from epigenetics to metabolism and therapeutics, Chem. Rev. 118 (2018) 1216–1252, https://doi.org/10.1021/acs.chemrev.7b00181.
[13] X.-J. Yang, E. Seto, Lysine acetylation: codified crosstalk with other posttranslational modifications, Mol. Cell 31 (2008) 449–461, https://doi.org/10.1016/j.molcel.2008.07.002.
[14] F. Hosp, I. Lassowskat, V. Santoro, et al., Lysine acetylation in mitochondria: from inventory to function, Mitochondrion 33 (2017) 58–71, https://doi.org/10.1016/j.mito.2016.07.012.
[15] N.S. Moretti, I. Cestari, A. Anupama, et al., Comparative proteomic analysis of lysine acetylation in trypanosomes, J. Proteome Res. 17 (2018) 374–385, https://doi.org/10.1021/acs.jproteome.7b00603.
[16] K.L. Norris, J.Y. Lee, T.P. Yao, Acetylation goes global: the emergence of acetylation biology, Sci. Signal. 2 (2009) pe76, https://doi.org/10.1126/scisignal.297pe76.
[17] A.K. Okada, K. Teranishi, M.R. Ambroso, et al., Lysine acetylation regulates the interaction between proteins and membranes, Nat. Commun. 12 (2021) 6466, https://doi.org/10.1038/s41467-021-26657-2.
[18] V. Bazylianska, H.A. Kalpage, J. Wan, et al., Lysine 53 acetylation of cytochrome c in prostate cancer: warburg metabolism and evasion of apoptosis, Cells 10 (2021), https://doi.org/10.3390/cells10040802.
[19] C. Choudhary, B.T. Weinert, Y. Nishida, et al., The growing landscape of lysine acetylation links metabolism and cell signalling, Nat. Rev. Mol. Cell Biol. 15 (2014) 536–550, https://doi.org/10.1038/nrm3841.

[20] J. Liu, C. Qian, X. Cao, Post-translational modification control of innate immunity, Immunity 45 (2016) 15–30, https://doi.org/10.1016/j.immuni.2016.06.020.
[21] M. Hui, J. Cheng, Z. Sha, First comprehensive analysis of lysine acetylation in *Alvinocaris longirostris* from the deep-sea hydrothermal vents, BMC Genom. 19 (2018) 352, https://doi.org/10.1186/s12864-018-4745-3.
[22] J. Lu, M. Zhang, H. Liang, et al., Comparative proteomics and transcriptomics illustrate the allograft-induced stress response in the pearl oyster (*Pinctada fucata martensii*), Fish Shellfish Immunol. 121 (2022) 74–85, https://doi.org/10.1016/j.fsi.2021.12.055.
[23] B. Allam, D. Raftos, Immune responses to infectious diseases in bivalves, J. Invertebr. Pathol. 131 (2015) 121–136, https://doi.org/10.1016/j.jip.2015.05.005.
[24] J. Cox, I. Matic, M. Hilger, et al., A practical guide to the MaxQuant computational platform for SILAC-based quantitative proteomics, Nat. Protoc. 4 (2009) 698–705, https://doi.org/10.1038/nprot.2009.36.
[25] G.R. Warnes, B. Bolker, L. Bonebakker, et al., Gplots: Various R Programming Tools for Plotting Data, vol. 2, 2009, p. 1.
[26] M.F. Chou, D. Schwartz, Biological sequence motif discovery using motif-x, Curr. Protoc. Bioinf. 35 (2011), https://doi.org/10.1002/0471250953.bi1315s35, 13.5.1-.5.24.
[27] B. MacLean, D.M. Tomazela, N. Shulman, et al., Skyline: an Open Source Document Editor for Creating and Analyzing Targeted Proteomics Experiments, vol. 26, 2010, pp. 966–968.
[28] X. Hu, Y. Yu, Y. Eugene Chin, et al., The role of acetylation in TLR4-mediated innate immune responses, Immunol. Cell Biol. 91 (2013) 611–614, https://doi.org/10.1038/icb.2013.56.
[29] X. Zhu, X. Liu, Z. Cheng, et al., Quantitative analysis of global proteome and lysine acetylome reveal the differential impacts of VPA and SAHA on HL60 cells, Sci. Rep. 6 (2016), 19926, https://doi.org/10.1038/srep19926.
[30] L. Lei, J. Zeng, L. Wang, et al., Quantitative acetylome analysis reveals involvement of glucosyltransferase acetylation in *Streptococcus mutans* biofilm formation, Environ. Microbiol. Rep. 13 (2021) 86–97, https://doi.org/10.1111/1758-2229.12907.
[31] Z.-K. Wang, Q. Cai, J. Liu, et al., Global insight into lysine acetylation events and their links to biological aspects in *Beauveria bassiana*, a fungal insect pathogen, Sci. Rep. 7 (2017), 44360, https://doi.org/10.1038/srep44360.
[32] X. Gu, Z. Hua, Y. Dong, et al., Proteome and acetylome analysis identifies novel pathways and targets regulated by perifosine in neuroblastoma, Sci. Rep. 7 (2017), 42062, https://doi.org/10.1038/srep42062.
[33] Y. Li, H. Li, M. Sui, et al., Fungal acetylome comparative analysis identifies an essential role of acetylation in human fungal pathogen virulence, Commun. Biol. 2 (2019) 154, https://doi.org/10.1038/s42003-019-0419-1.
[34] M. Zhao, S. Jia, X. Gao, et al., Comparative analysis of global proteome and lysine acetylome between naive CD4(+) T cells and CD4(+) T follicular helper cells, Front. Immunol. 12 (2021), 643441, https://doi.org/10.3389/fimmu.2021.643441.
[35] H. Li, J.D. Harwood, T. Liu, et al., Novel proteome and acetylome of Bemisia tabaci Q in response to *Cardinium* infection, BMC Genom. 19 (2018) 523, https://doi.org/10.1186/s12864-018-4907-3.
[36] Y. Li, H. Xue, D.-r. Bian, et al., Acetylome analysis of lysine acetylation in the plant pathogenic bacterium *Brenneria nigrifluens*, Microbiol. Open 9 (2020), e00952, https://doi.org/10.1002/mbo3.952.
[37] K.T. Smith, J.L. Workman, Introducing the acetylome, Nat. Biotechnol. 27 (2009) 917–919, https://doi.org/10.1038/nbt1009-917.
[38] I.H. Lee, T. Finkel, Regulation of autophagy by the p300 acetyltransferase, J. Biol. Chem. 284 (2009) 6322–6328.
[39] X. Fang, W. Chen, Y. Zhao, et al., Global Analysis of Lysine Acetylation in Strawberry Leaves, vol. 6, 2015, https://doi.org/10.3389/fpls.2015.00739.
[40] Y. Zhang, L. Song, W. Liang, et al., Comprehensive profiling of lysine acetylproteome analysis reveals diverse functions of lysine acetylation in common wheat, Sci. Rep. 6 (2016), 21069, https://doi.org/10.1038/srep21069.
[41] J. Pan, Z. Ye, Z. Cheng, et al., Systematic analysis of the lysine acetylome in *Vibrio parahemolyticus*, J. Proteome Res. 13 (2014) 3294–3302.
[42] D. Xu, X. Wang, Lysine acetylation is an important post-translational modification that modulates heat shock response in the sea cucumber, Apostichopus japonicus 20 (2019) 4423.
[43] M.P. Gupta, S.A. Samant, S.H. Smith, et al., HDAC4 and PCAF bind to cardiac sarcomeres and play a role in regulating myofilament contractile activity*, J. Biol. Chem. 283 (2008) 10135–10146, https://doi.org/10.1074/jbc.M710277200.
[44] S.A. Samant, V.B. Pillai, N.R. Sundaresan, et al., Histone deacetylase 3 (HDAC3)-dependent reversible lysine acetylation of cardiac myosin heavy chain isoforms modulates their enzymatic and motor activity, J. Biol. Chem. 290 (2015) 15559–15569, https://doi.org/10.1074/jbc.M115.653048.
[45] D.G. Guiney, M. Lesnick, Targeting of the actin cytoskeleton during infection by *Salmonella strains*, Clin. Immunol. 114 (2005) 248–255, https://doi.org/10.1016/j.clim.2004.07.014.
[46] A. Bitto, A.M. Wang, C.F. Bennett, et al., Biochemical Genetic Pathways that Modulate Aging in Multiple Species, vol. 5, 2015, a025114.
[47] H.S. Ban, T.-S. Han, K. Hur, et al., Epigenetic alterations of heat shock proteins (HSPs) in cancer, Int. J. Mol. Sci. 20 (2019), https://doi.org/10.3390/ijms20194758.
[48] Z. Wang, H. Liang, X. Du, et al., Cloning and express characters of HSP60 gene from *Pinctada martensii*, J. Guangdong Ocean Univ. 33 (2013) 14–23.
[49] B. Baron, Role of the post-translational modifications of HSP60 in disease, in: A.A. A. Asea, P. Kaur (Eds.), Heat Shock Protein 60 in Human Diseases and Disorders, Springer International Publishing, Cham, 2019, pp. 69–94, https://doi.org/10.1007/978-3-030-23154-5_6.
[50] X. Xiong, C. Li, Z. Zheng, et al., Novel globular C1q domain-containing protein (PmC1qDC-1) participates in shell formation and responses to pathogen-associated molecular patterns stimulation in *Pinctada fucata martensii*, Sci. Rep. 11 (2021) 1105, https://doi.org/10.1038/s41598-020-80295-0.
[51] L. Wang, C. Fan, W. Xu, et al., Characterization and functional analysis of a novel C1q-domain-containing protein in Japanese flounder *(Paralichthys olivaceus)*, Dev. Comp. Immunol. 67 (2017) 322–332, https://doi.org/10.1016/j.dci.2016.09.001.
[52] X. Liang, X. Xiong, Y. Cao, et al., Globular C1q domain-containing protein from *Pinctada fucata martensii* participates in the immune defense process, Fish Shellfish Immunol. 123 (2022) 521–527, https://doi.org/10.1016/j.fsi.2022.02.048.
[53] Q. Wang, Y. Liu, Z. Zheng, et al., Adaptive response of pearl oyster *Pinctada fucata martensii* to low water temperature stress, Fish Shellfish Immunol. 78 (2018) 310–315, https://doi.org/10.1016/j.fsi.2018.04.049.
[54] J. Zhang, X. Xiong, Y. Deng, et al., Integrated application of transcriptomics and metabolomics provides insights into the larval metamorphosis of pearl oyster (*Pinctada fucata martensii*), Aquaculture 532 (2021), 736067, https://doi.org/10.1016/j.aquaculture.2020.736067.
[55] G.L.J.T.J.o.c.i. Semenza, HIF-1 Mediates Metabolic Responses to Intratumoral Hypoxia and Oncogenic Mutations, vol. 123, 2013, pp. 3664–3671.
[56] X. Gao, H. Hong, W.-C. Li, et al., Downregulation of rubisco activity by non-enzymatic acetylation of RbcL, Mol. Plant 9 (2016) 1018–1027, https://doi.org/10.1016/j.molp.2016.03.012.
[57] O. Ozden, S.-H. Park, B.A. Wagner, et al., SIRT3 deacetylates and increases pyruvate dehydrogenase activity in cancer cells, Free Radic. Biol. Med. 76 (2014) 163–172, https://doi.org/10.1016/j.freeradbiomed.2014.08.001.
[58] H. Takeshi, A. Akira, Effect of air exposure on the acid–base balance of hemolymph in akoya pearl oyster (*Pinctada fucata martensii*), J. Shellfish Res. 40 (2022) 499–504, https://doi.org/10.2983/035.040.0306.